

Catalytic Ability of a Cationic Ru(II) Monochloro Complex for the Asymmetric Hydrogenation of Dimethyl Itaconate and Enamides

Isabel Serrano, Montserrat Rodríguez, and Isabel Romero*

Departament de Química, Universitat de Girona, Campus de Montilivi, E-17071 Girona, Spain

Antoni Llobet*

Departament de Química, Universitat Autònoma de Barcelona, Bellaterra, E-08193 Barcelona, Spain

Teodor Parella

Servei de RMN, Universitat Autònoma de Barcelona, Bellaterra, E-08193 Barcelona, Spain

Juan M. Campelo, Diego Luna,* and José M. Marinas

Departamento de Química Orgánica, Universidad de Córdoba, Campus de Rabanales, Edificio C3, E-14014 Córdoba, Spain

Jordi Benet-Buchholz

Institut Català d'Investigació Química (ICIQ), Països Catalans, 16, E-43007 Tarragona, Spain

Received June 23, 2005

The synthesis of two Ru chloro complexes, $\text{Ru}^{\text{II}}\text{Cl}_3(\text{bpea})$, **1**, and *cis-fac*- Δ -[$\text{Ru}^{\text{II}}\text{Cl}\{(R)\text{-}(\text{bpea})\}\{(S)\text{-}(\text{BINAP})\}$]-(BF_4), *cis-fac*- Δ -(*R*)-(S)-**2**, (bpea = *N,N*-bis(2-pyridylmethyl)ethylamine; (S)-BINAP = 2,2'-bis(diphenylphosphino)-1,1'-binaphthyl), is described. Complex **2** is characterized in solution through UV–vis, cyclic voltammetry (CV), and 1D and 2D NMR spectroscopy. X-ray diffraction analysis indicates that in the solid state it possesses the same structure as in solution, as expected for a low-spin d^6 Ru(II)-type complex. The molecular structure of *cis-fac*- Δ -(*R*)-(S)-**2**, consists of a nonsymmetric complex, where the Ru metal center has a significantly distorted octahedral-type coordination because of the bulkiness of the (S)-BINAP ligand. *cis-fac*- Δ -(*R*)-(S)-**2** has a remarkable catalytic performance at $P = 6.8$ atm of H_2 and $T = 70$ °C toward the hydrogenation of prochiral double bonds both from efficiency and from stereoselectivity viewpoints. As an example, prochiral olefins of technological interest such as dimethyl itaconate, methyl 2-acetamidoacrylate or methyl 2-acetamidocinnamate are catalytically hydrogenated by *cis-fac*- Δ -(*R*)-(S)-**2**, with conversions higher than 99.9% and ee > 99. Furthermore, *cis-fac*- Δ -(*R*)-(S)-**2**, also catalyzes the selective hydrogenation of β -keto esters, although the reaction rates are lower than those found with the former substrates.

Introduction

Asymmetric catalysis has become one of the most powerful tools in the production of a range of optically active compounds¹ that can be used, for instance, as intermediates

in the production of pharmaceutical drugs.² The use of transition metal complexes as asymmetric catalysts places

* To whom correspondence should be addressed. E-mail: marisa.romero@udg.es (I.R.); antoni.llobet@uab.es (A.L.).

- (1) (a) Sheldon, R. A. *Chirotechnology*; Marcel Dekker: New York, 1993. (b) Noyori, R. *Angew. Chem., Int. Ed.* **2002**, *41*, 2008–2022. (c) Noyori, R. *Adv. Synth. Catal.* **2003**, *345*, 15–32. (d) Genet, J.-P. *Acc. Chem. Res.* **2003**, *36*, 908–918.
(2) (a) Wadman, M. *Nature* **2001**, *410*, 615–616. (b) Ezzell, C. *Sci. Am.* **2000**, *283*, 98–103.

this exciting discipline at the interface of organic synthesis and inorganic chemistry.³

Asymmetric hydrogenation of prochiral ketones has been extensively studied using chiral diphosphine ligands such as BINAP. The specificity of Ru–BINAP catalysts has been documented by Noyori's group since the mid-1980s.⁴ Many ruthenium complexes have also been developed with the same purpose and with excellent performances containing chiral phosphines other than BINAP.⁵ At the moment, the asymmetric hydrogenation of substituted β -keto esters and prochiral dehydroamino acids is attracting a great deal of attention because they can be used as chiral building blocks in the design of pharmaceuticals, flavors, fragrances, and agrochemicals.⁶ Thus, together with dimethyl itaconate, those substrates constitute an excellent ground to test the catalytic performance of a given complex.

The asymmetric hydrogenation of dimethyl itaconate under mild conditions has mainly been achieved using Rh and Ru complexes generated in situ via the addition of a metal complex precursor and a monodentate or didentate chiral phosphine-type ligand.^{7,8} While for Rh complexes this strategy has led to impressive system performances with high efficiencies and enantiomeric excesses (close to or higher than 99%),⁷ for Ru complexes the performances of the systems are poorer, especially in regard to obtaining high enantiomeric excess under low hydrogen pressures.^{8–11} The lower enantiomeric excess performance displayed by Ru

complexes can, potentially, be attributed to their rich chemistry, given the extraordinary capacity of the Ru(II) transition metal to generate different types of complexes including different coordination environments, with or without the chiral ligand, as well as polynuclear-type complexes.¹² In addition, a recent report related to the kinetic influences on enantioselectivity¹³ is a further warning of the need to use perfectly characterized, single, discrete enantiopure complexes to understand system performance. However there are also some examples of isolated and completely characterized asymmetric Ru catalysts.^{11b}

Analogously, Rh catalysts containing chiral phosphine ligands have been successfully used as catalysts for the asymmetric hydrogenation of dehydroamino acids,¹⁴ but the corresponding Ru chemistry is still at its initial stages.¹⁵

In the present study, we wish to report the synthesis and the spectroscopic and structural characterization, both in the solid state and in solution, of a Ru complex, *cis-fac*- Δ -[Ru^{II}Cl{(R)-(bpea)}{(S)-(BINAP)}](BF₄), *cis-fac*- Δ -(R)-(S)-**2** (bpea = *N,N*-bis(2-pyridylmethyl)ethylamine; BINAP = 2,2'-bis(diphenylphosphino)-1,1'-binaphthyl). The performance of this complex in the homogeneous phase as a catalyst for the efficient and stereoselective hydrogenation of prochiral substrates, such as dehydroamino acids, dimethyl itaconate, and methyl acetoacetate, is disclosed.

Experimental Section

Materials. All reagents used in the present work were obtained from Aldrich Chemical Co and used without further purification. Reagent grade organic solvents were obtained from SDS, and high-purity deionized water was obtained by passing distilled water through a nano-pure Mili-Q water purification system. RuCl₃·2.4 H₂O was supplied by Johnson and Matthey Ltd. and was used as received.

Preparations. The bpea ligand, was prepared according to a literature procedure.¹⁶

All synthetic manipulations were routinely performed under a nitrogen atmosphere using Schlenk tubes and vacuum-line techniques.

Ru^{III}Cl₃(bpea)·2H₂O, 1·2H₂O. A 0.568 g (2.503 mmol) sample of bpea ligand was added to a magnetically stirred solution of

- (3) (a) Jacobsen, E.; Pfaltz, A.; Yamamoto, H. *Comprehensive Asymmetric Catalytic*; Springer: Heidelberg, Germany, 1999; Vol. 1–3. (b) Ojima, I. *Catalytic Asymmetric Synthesis*, 2nd ed.; Wiley: New York, 2000.
- (4) (a) Kitamura, M.; Ohkuma, T.; Inoue, S.; Sayo, N.; Kumobayashi, H.; Akutagawa, S.; Ohta, R.; Takaya, H.; Noyori, R. *J. Am. Chem. Soc.* **1988**, *110*, 629–631. (b) Noyori, R.; Ohkuma, T.; Kitamura, M.; Takaya, H.; Sayo, N.; Kumobayashi, H.; Akutagawa, S. *J. Am. Chem. Soc.* **1987**, *109*, 5856–5858.
- (5) (a) Michaud, G.; Bulliard, M.; Ricard, L.; Genet, J. P.; Marinetti, A. *Chem.—Eur. J.* **2002**, *8*, 3327–3330. (b) Gautier, I.; Ratovelomanana-Vidal, V.; Savignac, P.; Genet, J. P. *Tetrahedron Lett.* **1996**, *37* (43), 7721–7724. (c) Tranchier, J. P.; Ratovelomanana-Vidal, V.; Genet, J. P.; Tong, S.; Cohen, T. *Tetrahedron Lett.* **1997**, *38*, 2951–2954. (d) Bertus, P.; Phansavath, P.; Ratovelomanana-Vidal, V.; Genet, J. P.; Touati, A. R.; Homri, T.; Ben Hassine, B. *Tetrahedron: Asymmetry* **1999**, *10*, 1369–1380. (e) Blanc, D.; Ratovelomanana-Vidal, V.; Gillet, J. P.; Genet, J. P. *J. Organomet. Chem.* **2000**, *603*, 128–130. (f) Blanc, D.; Henry, J. C.; Ratovelomanana-Vidal, V.; Genet, J. P. *Tetrahedron Lett.* **1997**, *38*, 6603–6606. (g) Ohkuma, T.; Ooka, H.; Yamakawa, M.; Ikariya, T.; Noyori, R. *J. Org. Chem.* **1996**, *61*, 4872–4873.
- (6) (a) Fournie-Zaluski, M. C.; Coulaud, A.; Bouboutou, R.; Chaillet, P.; Devin, J.; Waksman, G.; Costentin, J.; Roques, B. P. *J. Med. Chem.* **1985**, *28*, 1158–1169. (b) Moore, W. M.; Spilburg, C. A. *Biochemistry* **1986**, *25*, 5189–5195. (c) Buhlmyer, P.; Caselli, A.; Fuhrer, W.; Goschke, R.; Rasetti, V.; Rueger, H.; Stanton, J. L.; Criscione, L.; Wood, J. M. *J. Med. Chem.* **1988**, *31*, 1839–1846. (d) Harada, H.; Yamaguchi, T.; Iyobe, A.; Tsubaki, A.; Kamijo, T.; Izuka, K.; Ogura, K.; Kiso, Y. *J. Org. Chem.* **1990**, *55*, 1679–1682. (e) Morimoto, T.; Chiba, M.; Achiwa, K. *Tetrahedron Lett.* **1990**, *31*, 261–264. (f) Burk, M. J.; Bienewald, F.; Harris, M.; Zanotti-Gerosa, A. *Angew. Chem., Int. Ed.* **1998**, *37*, 1931–1933.
- (7) (a) Christopfel, W. C.; Vineyard, B. D. *J. Am. Chem. Soc.* **1979**, *101*, 4406–4408. (b) Inoguchi, K.; Morimoto, T.; Achiwa, K. *J. Organomet. Chem.* **1989**, *370*, C9–C12. (c) Miyashita, A.; Karino, H.; Shimamura, J.; Chiba, T.; Nagano, K.; Nohira, H.; Takaya, H. *Chem. Lett.* **1989**, 1849–1852. (d) Burk, M. J.; Feaster, J. E.; Harlow, R. L. *Tetrahedron: Asymmetry* **1991**, *2*, 569–592. (e) Burk, M. J. *Acc. Chem. Res.* **2000**, *33*, 363–372.
- (8) Köckritz, A.; Bischoff, S.; Kant, M.; Siefken, R. *J. Mol. Catal. A* **2001**, *174*, 119–126.
- (9) Daley, C. J. A.; Wiles, J. A.; Bergens, S. H. *Can. J. Chem.* **1998**, *76*, 1447–1456.
- (10) (a) Noyori, R.; Ohta, M.; Hsiao, Y.; Kitamura, M.; Ohta, T.; Takaya, H. *J. Am. Chem. Soc.* **1986**, *108*, 7117–7119. (b) Ohta, T.; Takaya, H.; Kitamura, M.; Nagai, K.; Noyori, R. *J. Org. Chem.* **1987**, *52*, 3174–3176. (c) Matteoli, U.; Beghetto, V.; Scrivanti, A. *J. Mol. Catal. A* **1999**, *140*, 131–137.
- (11) (a) McCarthy, M.; Guiry, P. J. *Tetrahedron* **2001**, *57*, 3809–3844. (b) De Smet, K.; Pleyzier, A.; Vankelecom, I. F. J.; Jacobs, P. A. *Chem.—Eur. J.* **2003**, *9*, 334–338.
- (12) Housecroft, C. E.; Che, C. M.; Lau, T. C. *Comprehensive Coordination Chemistry II*; McCleverty, J. A., Meyer, T. J. Eds.; Elsevier Pergamon: Oxford, U.K., 2004, Vol. 5, Chapters 5.5 and 5.6, pp 555–847.
- (13) Blackmond, D. G.; Rosner, T.; Neugebauer, T.; Reetz, M. F. *Angew. Chem., Int. Ed.* **1999**, *38*, 2196–2199.
- (14) (a) Crépy, K. V. L.; Imamoto, T. *Adv. Synth. Catal.* **2003**, *345*, 79. (b) Jerphagnon, T.; Renaud, J. L.; Bruneau, C. *Tetrahedron: Asymmetry* **2004**, *15*, 2101.
- (15) (a) James, B. R.; Pacheco, A.; Rettig, S. J.; Thorburn, I. S.; Ball, R. G.; Ibers, J. A. *J. Mol. Catal.* **1987**, *41*, 147–161. (b) Wu, J.; Pai, C. C.; Kwok, W. H.; Guo, R. W.; Au-Yeung, T. L.; Yeung, C. H.; Chan, A. S. *Tetrahedron: Asymmetry* **2003**, *14*, 987–992.
- (16) Pal, S.; Chan, M. K.; Armstrong, W. H. *J. Am. Chem. Soc.* **1992**, *114*, 6398–6406.

$\text{RuCl}_3 \cdot 2.4\text{H}_2\text{O}$ (0.600 g (2.503 mmol) dissolved in dry MeOH (20 mL)), and then the mixture was refluxed for 1 h under Ar. Then it was allowed to cool to room temperature, and a brown solid precipitated; the solid was washed with MeOH and vacuum-dried. Yield: 0.68 g (60%). Anal. Found (Calcd) for $\text{C}_{14}\text{H}_{21}\text{Cl}_3\text{N}_3\text{RuO}_2$: C, 35.77 (35.71); H, 4.01 (4.30); N, 8.62 (8.92). IR (cm^{-1}): ν 3389 (O–H), 3051 (C–H), 2925 (C–H), 1608 (C=N), 1481, 1434, 1085, 999, 814, 743, 696 cm^{-1} .

cis-fac- Δ -[Ru^{II}Cl{(R)-(bpea)}{(S)-(BINAP)}](BF₄)·5H₂O, cis-fac- Δ -(R)-(S)-2·5H₂O. A 150 mg (0.32 mmols) sample of **1**·2H₂O and 40 mg (1.036 mmols) of LiCl were dissolved in 60 mL of 3:1 EtOH/H₂O under a nitrogen atmosphere. The resulting brown mixture was stirred for 10 min, and then 0.072 mL (0.517 mmols) of NEt₃ was added. The brown mixture was stirred for an additional 30 min, during which it turned dark green. At this point, 220 mg (0.35 mmols) of (S)-BINAP dissolved in 2 mL of EtOH were added, and the resulting solution was refluxed for 5 h. Then it was allowed to come to room temperature (approximately 22 °C), while a solid that mainly contained unreacted BINAP (approximately 150 mg; 68% of its initial amount) was filtered off the solution. Then 2 mL of a saturated aqueous solution of NaBF₄ was added to the filtered solution, and the volume was reduced in a rotary evaporator until a solid began to precipitate. At this point, the content was chilled overnight, forming a green solid. This green solid was filtered, washed with a small amount of cold water and ether, and air-dried. It was then purified by flash chromatography on an alumina column using CH₂Cl₂/CH₃CN (8:1) as eluent. Yield: 110 mg (29%). Anal. Found (Calcd) for $\text{C}_{58}\text{H}_{49}\text{BClF}_4\text{N}_3\text{P}_2\text{Ru} \cdot 5\text{H}_2\text{O}$: C, 59.75 (59.88); H, 5.09 (5.11); N, 3.90 (3.61). IR: ν 3370 (O–H), 3052 (C–Har), 1434 (C=N), 1086, 696 cm^{-1} . ¹H NMR (CD₂Cl₂, 500.13 MHz, 190 K): δ 9.13 (t, 1, H₁₆), 9.0 (d, 1, H₁₁), 8.65 (t, 1, H₄₈), 8.30 (t, 1, H₂₈), 7.82 (d, 1, H₂₉), 7.75 (t, 1, H₄₅), 7.71 (d, 1, H₃₁), 7.61 (d, 1, H₄₄), 7.53 (d, 1, H₄₂), 7.47 (t, 1, H₁₈), 7.41 (m, 1, H₅₅), 7.40 (d, 1, H₁₃), 7.39 (d, 1, H₁₉), 7.33 (m, 1, H₂₀), 7.32 (m, 1, H₁₇), 7.29 (m, 1, H₇), 7.23 (m, 2, H₂₂, H₄₁), 7.18 (m, 2, H₈, H₅₄), 7.15 (d, 1, H₃₂), 7.14 (m, 1, H₂₆), 7.05 (t, 1, H₅₂), 6.97 (t, 1, H₅₁), 6.89 (t, 1, H₅₇), 6.85 (t, 1, H₁₂), 6.83 (d, 2, H₅₀, H₅₆), 6.76 (d, 1, H₅₈), 6.70 (d, 1, H₄₀), 6.68 (d, 1, H₁₄), 6.61 (d, 1, H₅), 6.47 (t, 1, H₄₉), 6.41 (t, 1, H₃₃), 6.11 (t, 1, H₆), 5.70 (d, 1, H₃₉), 5.47 (d, 1, H₃₄), 5.09 (d, 1, H_{3a}), 4.21 (d, 1, H_{3b}), 4.11 (dd, 1, H_{1a}), 3.74 (d, 1, H_{9b}), 3.29 (d, 1, H_{1b}), 1.99 (s, 1, H_{9a}), 0.97 (t, 3, H₂). ¹³C NMR (CD₂Cl₂, 500.13 MHz, 190 K): δ 157.1 (C11), 152.8 (C5), 139.8 (C16), 137.8 (C48), 137.2 (C17), 136.9 (C52), 136.5 (C13), 135.9 (C58), 134.9 (C22), 134.3 (C20), 133.2 (C8), 130.6 (C18), 130.0 (C12), 129.9 (C19), 129.7 (C55), 128.8 (C7), 128.6 (C28), 128.4 (C44), 127.6 (C42), 127.2 (C39, C41, C57), 127.1 (C51), 126.9 (C31), 126.6 (C49), 126.3 (C34), 126.2 (C32), 125.7 (C40), 125.6 (C45), 125.3 (C33), 125.0 (C29), 124 (C50, C56), 122.8 (C14), 122.4 (C54), 122.2 (C6), 66.9 (C3), 64.7 (C9), 59.5 (C1), 7.9 (C2). ³¹P NMR (CD₂Cl₂, 202.45 MHz, 200 K): δ 27.8 (d, $J_{\text{P1-P2}} = 50.6$ Hz, P₂), 42.8 (d, P₁). ROEs: H1a with 1b, 2, 9a, 3a, 8, 48; H1b with 1a, 2, 9a, 3a, 14, 8; H2 with 1b, 9b, 1a, 3b, 3a; H3a with 1b, 1a, 3b, 8; H3b with 2, 9b, 3a, 8; H5 with 11; H9a with 1b, 9b, 1a; H9b with 2, 9a, 1b, 3b, 14; H11 with 5, 58, 12, 54, 8; H16 with 49, 7; H28 with 20, 29; H34 with 39, 33, 51, 52; H39 with 33, 34, 40, 26, 41; H48 with 1a, 49; H51 with 34; H52 with 34; H58 with 45. $E_{1/2}$ (CH₂Cl₂ + 0.1 M TBAH): 1.10 V vs SSCE. UV–vis (CH₃CN, 2×10^{-4} M) λ_{max} (ϵ): 221 (56 660), 331 sh (5550), 365 nm (4150 M⁻¹ cm⁻¹).

For NMR assignment, we have used the same labeling scheme used for the crystal structure shown in Figure 1 and in Scheme 1.

Instrumentation and Measurements. IR spectra were recorded on a MKII Golden Gate Single Reflection ATR System. UV–vis spectroscopy was performed on a Cary 50 Scan (Varian) UV–vis

spectrophotometer with 1 cm quartz cells. Cyclic voltammetric (CV) experiments were performed in a PAR 263A EG&G potentiostat or an IJ-Cambria IH-660 using a three electrode cell. Glassy carbon disk electrodes (3 mm diameter) from BAS were used as working electrodes; platinum wire was used as the auxiliary electrode, and SSCE was used as the reference electrode. All cyclic voltammograms presented in this work were recorded under a nitrogen atmosphere. The complex was dissolved in previously degassed solvents containing the necessary amount of $n\text{-Bu}_4\text{N}^+\text{PF}_6^-$ (TBAH). All $E_{1/2}$ values reported in this work were estimated from cyclic voltammetry as the average of the oxidative and reductive peak potentials, $(E_{\text{p,a}} + E_{\text{p,c}})/2$. Unless explicitly mentioned, the concentration of the complexes was approximately 1 mM.

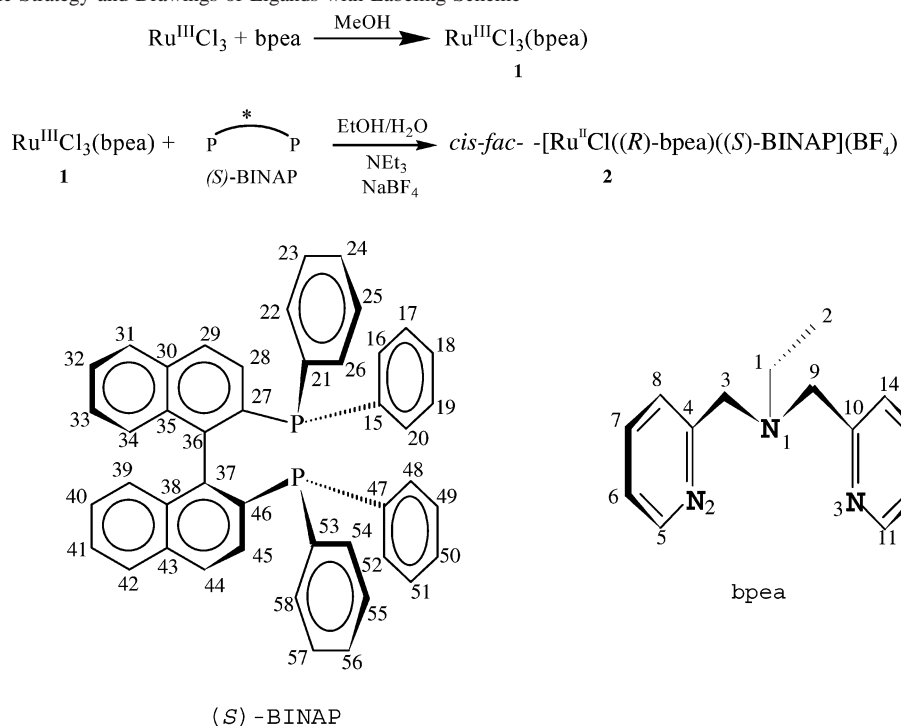
Catalytic hydrogenation activity measurements were performed in a conventional low-pressure hydrogenator (Parr Inst. Co., Mod.3911) at controlled pressure and temperature conditions. Hydrogenation runs were accomplished in methanol, as solvent, with 20 mL of 0.80 M substrate solution with 0.034 g of *cis-fac- Δ -(R)-(S)-2·5H₂O* (Scheme 1) to obtain $[\text{subs}]/[\text{cat}] = 0.016/0.000029 = 547$. In all cases, initial hydrogen pressure was 6.8 atm, and temperatures were in the range of 50–70 °C. Methanol (99%, Scharlau) and hydrogen (99.999% SEO) were used without further purification. Methyl acetoacetate and 1-hexene were used as supplied by Merck, after distillation under reduced pressure and low temperature. Dimethyl itaconate and methyl 2-acetamidocrylate were used as supplied by Aldrich, and methyl 2-acetamidocinnamate was synthesized by esterification of the corresponding 2-acetamidocinnamic acid (Aldrich), by refluxing it with a boron trifluoride-methanol complex (Merck).^{17a} The analyses of hydrogenation products were performed on a Konik-3000 gas chromatograph equipped with a Supelco (BETA DEX 120) β -cyclodextrin chiral column. Reaction rates and turnover frequencies (TOF_{max}) were calculated from the initial reaction rates. Those were obtained from a least-squares fit of the slopes of the plots of the initial linear decrease in hydrogen pressure versus reaction time. Since these plots were always practically linear up to 70–90% conversion, the determination of initial rates was straightforward. Absolute configuration and ee were obtained from the rotary power of samples measured with a P20 polarimeter (Bellingham & Stanley LTD) and confirmed by the absolute configuration of authentic samples assigned in the GC peaks. In this respect, dimethyl (R)-(+)-methylsuccinate, $[\alpha]_{\text{D}}^{20} = +11.0^\circ$ ($c = 1$, CHCl₃), and methyl (R)-3-hydroxybutyrate, $[\alpha]_{\text{D}}^{20} = -50.0^\circ$ ($c = 1.3$, CHCl₃), were obtained from Aldrich. The methyl ester of *N*-acetyl-(S)-phenylalanine was synthesized by esterification of the corresponding *N*-acetyl-(S)-phenylalanine (Aldrich), by refluxing it with the boron trifluoride-methanol complex (Merck),^{17a} $[\alpha]_{\text{D}}^{20} = +18.3^\circ$ ($c = 8$, CH₂Cl₂). To obtain the methyl esters of *N*-acetyl-(S)-alanine, it was also necessary to synthesize *N*-acetyl-(S)-alanine via the acetylation of alanine (Aldrich) with acetic anhydride^{17b} before the esterification process,^{17a} $[\alpha]_{\text{D}}^{20} = +14.8^\circ$ ($c = 4$, CH₂Cl₂).

The NMR spectroscopy was performed on a Bruker 500 MHz spectrometer. Samples were run in CD₂Cl₂. Elemental analyses were performed using a CHNS–O elemental analyzer (EA-1108) from Fisons.

X-ray Structure Determination. Single crystals were grown by slow diffusion of ether into a CH₂Cl₂ solution. Crystal structure determination was carried out using a Siemens P4 diffractometer equipped with a SMART-CCD-1000 area detector, a MACScience

(17) (a) Vogel, A. I. *Vogel's Text Book of Practical Organic Chemistry*, 4th ed.; Longman Group Limited: London, 1989; p 1079. (b) Vogel, A. I. *Vogel's Text Book of Practical Organic Chemistry*, 4th ed.; Longman Group Limited: London, 1989; p 1273.

Scheme 1. Synthetic Strategy and Drawings of Ligands with Labeling Scheme



Co. rotating anode with Mo K α radiation, a graphite monochromator, and a Siemens low-temperature device LT2 ($T = -120\text{ }^\circ\text{C}$). Full-sphere data collection included ω and ϕ scans. The programs used were as follows: data collection, Smart, version 5.060 (Bruker AXS, 1999); data reduction, Saint+, version 6.02 (Bruker AXS, 1999); and absorption correction, SADABS (Bruker AXS 1999). Crystal structure solution was achieved using direct methods as implemented in SHELXTL, version 5.10 (Sheldrick, Universität Göttingen, Germany, 1998) and visualized using the XP program. Missing atoms were subsequently located from difference Fourier synthesis and added to the atom list. Least-squares refinement on F^2 using all measured intensities was carried out using the program SHELXTL, version 6.10 (Sheldrick, Universität Göttingen, Germany, 2000). All non-hydrogen atoms were refined including anisotropic displacement parameters. The water molecules are mostly crystallographically disordered and localized in 10 positions.

Results and Discussion

Synthesis, Structure, and Stereoisomeric Analysis. The addition of bpea to a methanolic solution of $\text{RuCl}_3 \cdot \text{H}_2\text{O}$ produces $[\text{Ru}^{\text{III}}\text{Cl}_3(\text{bpea})]$, **1**, in moderate yields. The reduction of complex **1** with NEt_3 , followed by addition of (*S*)-BINAP, generates the *cis-fac*- Δ -(*R*)-(*S*)-**2** complex in a 29% yield (Scheme 1). The low yield is the result of the bulkiness of the (*S*)-BINAP ligand that, as a consequence, remains unreacted.¹⁸ A very small amount of impurities were removed by simple column chromatography over alumina. The exclusive formation of the *cis-fac*- Δ -(*R*)-(*S*)-**2** complex in a diastereoselective manner is due to the structure and bulkiness of both the (*S*)-BINAP and bpea ligands (vide infra).

The crystal structure of the chiral compound *cis-fac*- Δ -(*R*)-(*S*)-**2**·6H₂O¹⁹ has been solved by X-ray diffraction analysis. Figure 1 presents the ORTEP diagram for the cationic moiety, and the crystallographic data and selected bond distances and angles are included in Tables 1 and 2, respectively. The molecular structure of **2** shows an unsymmetric complex where the Ru metal atom presents a highly distorted octahedral geometry with the bpea ligand facially coordinated through its nitrogen atoms and the (*S*)-BINAP ligand acting in a chelate manner through its P atoms forming a highly skewed seven-member ring structure that determines the chiral disposition of the four phenyl rings on the phosphorus atoms; two phenyls are oriented in axial directions, while the other two are oriented in equatorial directions forming the so-called quadrangular arrangement²⁰ (the equatorial plane is defined from now on as the best plane that contains RuP1P2N1 and N2 and is nearly perpendicular to the Ru–Cl bond). The final coordination position is occupied by the chloro ligand which is situated *cis* to the aliphatic N atom of the bpea ligand and the P atoms of the (*S*)-BINAP ligand (the Cl ligand could also be situated *trans* to the N atom, thus the nomenclature adopted by **2**). Bond distances and angles for this complex are within the values previously reported for this type of complex.^{21,22}

The steric effects of the bulkiness of the (*S*)-BINAP and bpea ligands produce a distortion of the equatorial plane

(18) Long refluxing times are required for BINAP coordination compared with that of nonbulky ligands, for instance, see: Llobet, A.; Doppelt, P.; Meyer, T. J. *Inorg. Chem.* **1988**, *27*, 514–520.

(19) *S* refers to the configuration of the BINAP ligand that does not change during the coordination process; *R* refers to the configuration of the aliphatic N atom of the bpea ligand that becomes chiral upon coordination, since both arms in the bpea ligand can be distinguished through their respective different trans ligands in the complex structure; the Δ term is obtained by considering (1) the chelate BINAP ligand and (2) the chelate ring involving N1 and N3 in the bpea ligand.

(20) Noyori, R.; Kitamura, M.; Ohkuma, T. *Proc. Natl. Acad. Sci. U.S.A.* **2004**, *101*, 5356–5362.

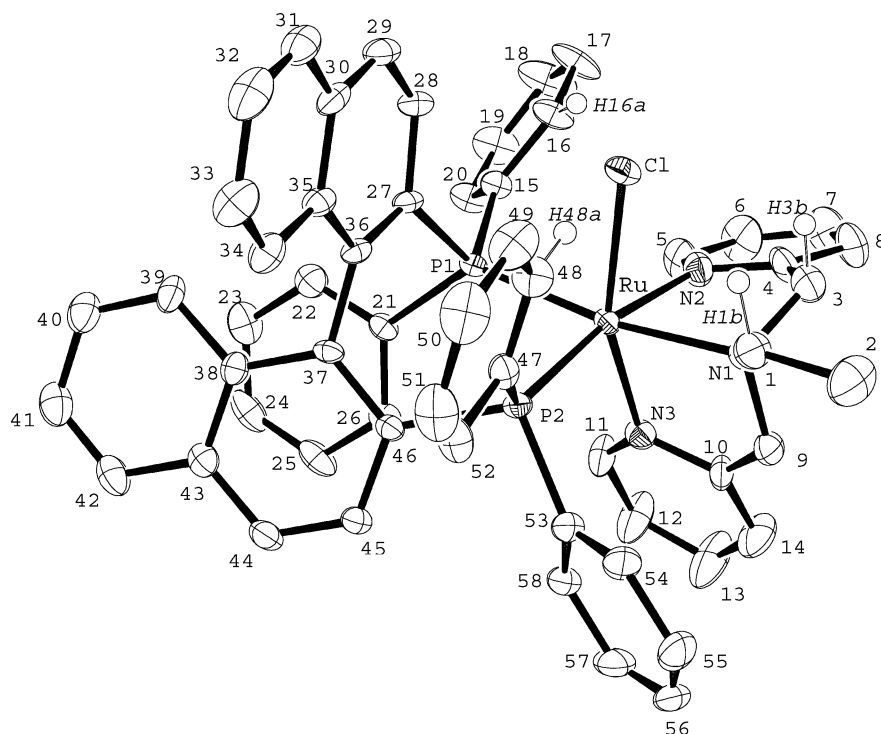


Figure 1. ORTEP plot (ellipsoids drawn at the 30% probability level) with labeling scheme for the cationic moiety of the *cis-fac-Δ(R)-(S)-2* complex.

Table 1. Crystal Data for *cis-fac-Δ(R)-(S)-2*·6H₂O

empirical formula	C ₅₈ H ₄₉ B ₁ Cl ₁ F ₄ N ₃ O ₆ P ₂ Ru ₁
fw	1169.27
cryst syst, space group	triclinic, <i>P</i> $\bar{1}$
<i>a</i> (Å)	11.4506(4)
<i>b</i> (Å)	11.4944(4)
<i>c</i> (Å)	12.1990(3)
α (deg)	102.217(2)
β (deg)	105.351(10)
γ (deg)	111.9790(10)
<i>V</i> (Å ³)	1346.3(7)
formula units/cell	1
ρ_{calcd} (g cm ⁻³)	1.452
μ (mm ⁻¹)	0.468
final <i>R</i> ^a , <i>wR</i> ^b [<i>I</i> > 2 σ (<i>I</i>)]	0.0527, 0.1284

^a $R_1 = \sum ||F_o| - |F_c|| / \sum |F_o|$. ^b $wR_2 = [\sum \{w(F_o^2 - F_c^2)^2\} / \sum \{w(F_o^2)^2\}]^{1/2}$, where $w = 1/[\sigma^2(F_o^2) + (0.0042P)^2]$ and $P = (F_o^2 + 2F_c^2)/3$.

generating a dihedral angle of 10.5° between the planes containing RuP1P2 and RuN1N2. The bulkiness of these two ligands is also manifested by a remarkable distortion of Ru–Cl bond away from the (*S*)-BINAP ligand with an N3Ru1Cl1 trans angle of 159.7° (more than 20° degrees below the ideal 180°). The geometrical situation of the Cl ligand is also interesting because it is intramolecularly hydrogen bonded with both the (*S*)-BINAP and bpea ligands. Two relatively strong hydrogen bonds are present with the H48a and H16a atoms (C48–H48a = 0.950 Å, H48a–Cl1 = 2.436 Å, C48–Cl1 = 3.343 Å, C48–H48a–Cl1 = 159.6°; C16–H16a =

Table 2. Selected Bond Distances and Angles for *cis-fac-Δ(R)-(S)-2*

Ru1–N3	2.091(3)	N3–Ru1–N2	76.74(16)
Ru1–N2	2.161(4)	N3–Ru1–N1	80.79(15)
Ru1–N1	2.208(5)	N2–Ru1–N1	106.82(12)
Ru1–P1	2.3397(12)	N2–Ru1–P1	99.04(12)
Ru1–P2	2.3619(11)	N1–Ru1–P1	171.21(10)
Ru1–Cl1	2.4227(10)	N3–Ru1–P2	95.73(11)
		N2–Ru1–P2	170.20(11)
		N1–Ru1–P2	94.57(11)
		P1–Ru1–P2	89.10(4)
		N3–Ru1–Cl1	159.81(12)
		N2–Ru1–Cl1	86.13(12)
		N1–Ru1Cl1	85.35(10)
		P1–Ru1–Cl1	86.15(4)
		P2–Ru1–Cl1	99.96(4)

0.949 Å, H16a–Cl1 = 2.526 Å, C16–Cl1 = 3.364 Å, C16–H16a–Cl1 = 147.2°) of the phenyl rings that are situated above the equatorial plane, while two more medium strength hydrogen bonds are formed with the H1b and H3b atoms (C1–H1b = 0.991 Å, H1b–Cl1 = 2.726 Å, C1–Cl1 = 3.349 Å, C1–H1b–Cl1 = 121.2°; C3–H3b = 0.990 Å, H3b–Cl1 = 2.700 Å, C3–Cl1 = 3.196 Å, C3–H3b–Cl1 = 111.3°) of two methylene groups of the bpea ligand. This special relative disposition of the (*S*)-BINAP and bpea ligands is very important because it determines the size and shape of the active site chiral pocket of this particular molecule.

The bpea ligand is a flexible molecule that can potentially act either in a meridional^{21b} or facial fashion^{21b,23} when coordinating a transition metal. In the presence of the (*S*)-BINAP ligand, the former type of coordination would lead to two highly disfavored isomers because of the strong steric repulsion that would generate the upper naphthyl ring (the

(21) (a) Romero, I.; Rodríguez, M.; Llobet, A.; Collomb, M. N.; Deronzier, A.; Parella, T.; Stoeckli-Evans, H. *J. Chem. Soc., Dalton Trans.* **2000**, 1689–1694. (b) Rodríguez, M.; Romero, I.; Llobet, A.; Dereonzier, A.; Biner, M.; Parella, T.; Stoeckli-Evans, H. *Inorg. Chem.* **2001**, *40*, 4150–4156. (c) Sens, C.; Romero, I.; Rodríguez, M.; Llobet, A.; Parella, T.; Benet-Buchholz, J. *J. Am. Chem. Soc.* **2004**, *126*, 7798–7799.

(22) Chan, A. S.; Laneman, S. A.; Day, C. X. *Inorg. Chim. Acta* **1995**, *228*, 159–163.

(23) Pal, S.; Olmstead, M. M.; Armstrong, W. H. *Inorg. Chem.* **1995**, *34*, 4708–4715.

one that contains the C27–C36 carbon atoms) with the upper pyridyl ring of the bpea or the upper C47–C52 phenyl ring with the aliphatic N atom trans to P1 or P2. Acting in a facial manner, the bpea ligand can coordinate either cis or trans with regard to the relative disposition of the Cl and N aliphatic atoms of bpea. The trans isomer is highly disfavored in our case because one of the bpea pyridyl rings would have a strong steric repulsion with the lower equatorial (*S*)-BINAP phenyl C53–C58 ring. The bpea ligand is a symmetric ligand and thus does not present chirality, but in a cis-fac-type coordination, the two pyridylic arms can be considered different if their bonding trans counterparts are different, which is the case. Thus, the aliphatic N atom becomes chiral upon coordination and adopts an R conformation. Because the whole molecule does not have any element of symmetry, this Ru complex is also chiral, adopting a Δ conformation. The corresponding *cis-fac* Δ -(*S*)-(S)-**2** isomer would also be highly disfavored because of the steric interaction of one of the pyridylic rings of bpea with, again, the lower equatorial (*S*)-BINAP phenyl C53–C58 ring.

Spectroscopic and Redox Properties. The 1D and 2D NMR spectra of *cis-fac*- Δ -(*R*)-(S)-**2** were registered in CD₂Cl₂, and all resonances can be unambiguously assigned by careful examination of 2D COSY and 2D NOESY/ROESY spectra. Table S1 (Supporting Information) shows the ¹H and ¹³C NMR assignments, together with the most relevant NOE enhancements observed in the ROESY spectrum at 190 K. The complete stereospecific proton assignments of the complex aromatic region was performed by careful analysis of ROESY data, allowing the identification of individual Ph–P orientations from the different anisotropic chemical shift properties of all nonequivalent resonances (Figure S2). Enlargements for 1D NMR spectra, together with other 2D spectra, are shown as Supporting Information (Figures S3–S6).

Solution NMR spectroscopy of *cis-fac*- Δ -(*R*)-(S)-**2** is also in agreement with the presence of this isomer only, and the unusual downfield shift of the H48a, H16a, H1b and H3b resonances, which is consistent with the hydrogen bonding to the chloro ligand described in the previous section, is worth mentioning here. The asymmetry of the compound is also reflected by the AX spin system in the ³¹P NMR spectrum (Figure S9 in the Supporting Information), with two doublets resonating at 42.8 and 27.8 ppm corresponding to the P(1) and P(2) atoms, respectively, of the (*S*)-BINAP ligand. These ³¹P resonances were assigned by concerted use of long-range through-bond ¹H–³¹P data obtained from an HMBC spectrum and the interligand NOE contacts observed between the Ph(BINAP) and the bpea moieties.

Many aromatic ¹H resonances belonging to the four (*S*)-BINAP phenyl rings are completely missing at 298 K because of the restricted P–Ph bond rotation in the complex, a feature that has been already reported for related BINAP-containing complexes²⁴ (Figure S1). This dynamic behavior was also confirmed by the strong chemical exchange peaks

observed in both the NOESY and ROESY spectra at several temperatures ranging from 220 to 300 K. Sharp line widths and no exchange contributions were achieved at 190 K for three out of four of the (*S*)-BINAP phenylic rings. For the two upper rings (C47–C52 and C15–C20), the P–Ph rotation is slowed because of the formation of the hydrogen bonds with the chloro ligand, whereas for the lower phenyl ring (C53–C58), the rotation is restricted because of the close presence of the bpea pyridylic ring containing the N3 atom. In sharp contrast, the fourth phenyl ring (C21–C26) is allowed to rotate freely without the restrictions described above for the other three rings, and thus its ortho and meta hydrogen atoms could not be distinguished.

The electronic spectrum of chloro complex **2** is shown in figure S7, and the corresponding λ_{max} and ϵ values are given in the Experimental Section. The complex presents ligand-based π – π^* transitions below 300 nm probably overlapping the less intense Ru(II) to phosphine ligand charge-transfer (CT) bands.²⁵ A band at 365 nm can be assigned to a MLCT $d\pi$ – π^* (Ru–bpea);^{20b} this band is shifted to higher energy when compared to the analogous band for [Ru(Cl)(bpea)(bpy)]⁺ (bpy is 2,2'-bipyridine), which appears at 380 nm. This phenomenon is associated with the stabilization of $d\pi$ Ru orbitals when bpy is replaced by a stronger π -acid such as the diphosphine (*S*)-BINAP ligand.

Redox properties were investigated by means of cyclic voltammetry (CV). The CV of *cis-fac*- Δ -(*R*)-(S)-**2** in CH₂Cl₂ exhibits a quasireversible oxidation wave at $E_{1/2} = 1.10$ V vs SSCE, corresponding to the Ru^{III}/Ru^{II} redox couple ($\Delta E_p = 130$ mV, 100 mV s⁻¹ scan rate). This wave is shifted anodically by 362 mV when compared to the Ru(III)/Ru(II) couple of [Ru(Cl)(bpea)(bpy)]⁺ ($E_{1/2} = 0.738$ V). This anodic shift is also consistent with higher π -acceptor ability of the (*S*)-BINAP ligand, compared to that of the bpy ligand, which stabilizes $d\pi$ Ru orbitals.²⁶


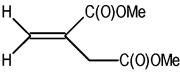
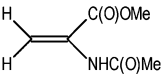
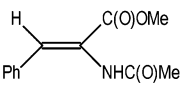
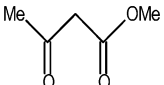
Catalytic Properties. The capacity of *cis-fac*- Δ -(*R*)-(S)-**2** to catalyze the enantioselective hydrogenation of prochiral olefinic double bonds in some molecules of technological interest was evaluated (hydrogen pressure of 6.8 atm, $T = 70$ °C, [cat]/[subs] = 1/547), and the results obtained are shown in Tables 3 and 4. Those tables also contain the TOF values, obtained from the initial reaction rates, reaction times, and conversions, as well as the half-reaction times, corresponding to the amount of time (in hours) necessary to carry out the 50% substrate conversion. While the TOFs are highly reproducible (see Tables 3 and 4 for dimethyl itaconate), the time for the total consumption of the substrate and the half-reaction times differ a little as expected for these type of measurements. Further, the rotary power of the products were always coincidental with the pure samples, and no GC traces of the complementary enantiomers were obtained; this is thus indicative that greater than a 99% ee was obtained in all cases. Table 3 shows the remarkable performance of *cis*-

(24) (a) Geldbach, T. J.; Rügger, H.; Pregosin, P. S. *Magn. Reson. Chem.* **2003**, *41*, 703–708. (b) Deeming, A. J.; Speel, D. M.; Stchedroff, M. *Organometallics* **1997**, *16*, 6004–6009.

(25) Sullivan, B. P.; Salmon, D. J.; Meyer, T. J. *Inorg. Chem.* **1978**, *17*, 3334–3341.

(26) (a) Batista, A. A.; Polato, E. A.; Queiroz, S. L.; Nascimento, O.; James, B. R.; Rettig, S. J. *Inorg. Chim. Acta* **1995**, *230*, 111–117. (b) Dovelotoglou, A.; Adeyemi, S. A.; Meyer, T. J. *Inorg. Chem.* **1996**, *35*, 4120–4127.

Table 3. Catalytic Performance of *cis-fac*- Δ -(*R*)-(*S*)-**2** Toward the Hydrogenation of 1-Hexene and Some Prochiral Olefins^a

Substrate	Product	Initial Reac. Rate ^b (μ mol/ s)	TOF _{max} ^b (h ⁻¹)	Half Reac. ^c (h)	Cons. Time ^d (h)	Conv. (%)	ee
1-Hexene 	Hexane	0.254	28.6	10.0	37.0	> 99.9	_
Dimethyl itaconate 	Dimethyl (<i>R</i>)-methylsuccinate	0.250	28.2	11.0	38.0	> 99.9	> 99
Methyl 2-acetamidoacrylate 	Methyl <i>N</i> -acetyl- (<i>S</i>)-alanine	0.821	105.8	2.5	10.0	> 99.9	> 99
Methyl 2-acetamidocinnamate 	<i>N</i> -Acetyl-(<i>S</i>)-phenylalanine	0.036	4.1	105.0	313.0	> 99.9	> 99
Methyl acetoacetate 	Methyl (<i>R</i>)-3-hydroxybutyrate	0.016	1.8	146.0	300.0	71.1	> 99

^a Thirty-four milligrams (29.2 μ mol) of *cis-fac*- Δ -(*R*)-(*S*)-**2**·5H₂O and 16.0 mmol of substrate ([subs]/[cat] = 547) dissolved in 20 mL of methanol. Hydrogen pressure 6.8 atm and $T = 70$ °C. ^b See Experimental Section for calculation details, product quantification, and identification procedures. ^c Half Reac., the half-reaction time, is defined as the amount of time (in hours) needed for the consumption of 50% of the substrate. ^d Cons. Time, consumption time, is defined as the amount of time (in hours) needed for total consumption of the substrate.

Table 4. Successive Homogeneous Asymmetric Hydrogenation of Dimethyl Itaconate to Dimethyl (*R*)-Methylsuccinate Using *cis-fac*- Δ -(*R*)-(*S*)-**2**^a

run	T (°C)	initial reaction rate (μ mol/s)	TOF _{max} (h ⁻¹)	half reac. ^c (h)	cons. time ^c (h)
1	70.0	0.252	28.4	9.0	29.0
2	70.0	0.263	29.6	10.0	31.0
3	65.0	0.156	17.6	15.0	45.0
4	60.0	0.132	14.8	19.0	52.0
5	55.0	0.065	7.3	35.0	122.0
6	50.0	0.031	3.5	73.0	144.0
7	70.0	0.160	16.5	16.0	48.0
8	70.0	0.146	18.5	20.0	48.0
9	70.0	0.123	13.8	27.0	55.0
10	70.0	0.099	11.1	39.0	64.0
11	70.0	0.066	7.4	42.0	71.0
12	70.0	0.046	4.7	61.0	98.0
13	70.0	0.024	2.5	90.0	144.0
14	70.0	0.031	3.2	82.0	168.0 ^b

^a Same reaction conditions as in Table 3. In all cases 99.9% conversion is attained with ee > 99. ^b Overall TON = 6384 metal cycles during 1119 h (46.6 days) of continuous catalytic reaction. ^c See text and Table 3 for definitions.

fac- Δ -(*R*)-(*S*)-**2** with regard to its ability to efficiently and asymmetrically hydrogenate dimethyl itaconate, methyl 2-acetamidoacrylate, and methyl 2-acetamidocinnamate. In

the case of a β -dicarboxylic compound, such as methyl acetoacetate, it displays moderate activity but maintains its stereoselectivity. Finally, it does not react with acetophenone under these conditions. To determine the overall turnover number (TON) of the catalyst, several successive reactions were carried out at different temperatures, in a continuous manner, meaning that successive amounts of the dimethyl itaconate substrate (0.016 mol in 5 mL of methanol) were introduced to the reactor vessel after the previous hydrogenation reaction had finished (so that successive amounts of hydrogenated substrate are accumulated in the vessel along the process), until the catalyst was deactivated. Thus, the catalyst used in each successive step is always the initial *cis-fac*- Δ -(*R*)-(*S*)-**2** introduced in the first run (0.034 g), and so, at the end of the fourteen successive reactions, we have in the vessel 35.8 g of dimethyl (*R*)-methylsuccinate, together with the catalyst, in 90 mL of methanol solution. Table 4 shows the results obtained for this series of reactions, and as can be seen, the catalyst slowly deactivates resulting smaller reaction rates. However, it always generates enantiomerically pure dimethyl (*R*)-methylsuccinate (ee > 99%) with a complete conversion. For example, on the 14th run

Cationic Ru(II) Monochloro Complex

the initial rate has dropped to 0.031 $\mu\text{mol/s}$, while the overall number of metal cycles reaches a value of 6384.

From a mechanistic perspective, it is interesting to observe the sharp decrease of the initial reaction rate caused by an increase of the steric encumbrance, as exemplified by the methyl 2-acetamidoacrylate (821 nmols/s) versus methyl 2-acetamidocinnamate (36 nmols/s) substrates. From this same perspective, it is also of interest to determine if both ligands, (*S*)-BINAP and bpea, remain rigidly bonded or if at some point one of the N or P atoms could decoordinate. A thorough mechanistic analysis is currently underway.

Acknowledgment. This research has been financed by MCYT of Spain through Projects CTQ2004/021662-E, CTQ2004-02200/BQU, CTQ2005/04080/BQU, BQU2003-

02884, BQU2003-01677, and BQU2001-2605. We thank also CIRIT Generalitat de Catalunya (Spain) for the Distinction award (A.L.) and for aid (SGR2001-UG-291). The financial support of the Junta de Andalucía, FEDER funds, and Johnson and Matthey for a $\text{RuCl}_3 \cdot 2.4 \text{H}_2\text{O}$ loan are also acknowledged.

Supporting Information Available: Additional spectroscopic data for *cis-fac*- Δ -(*R*)-(*S*)-**2**, as well as the CIF file with the crystallographic information. This material is available free of charge via the Internet at <http://pubs.acs.org>. Crystallographic information has been deposited with the Cambridge Crystallographic Data Centre (CCDC 252121).

IC051032W